Explicit transformation between non-adhesive and adhesive contact problems by means of the classical JKR formalism

Nikolay V. Perepelkin[1,*] and Feodor M. Borodich[2]

[1]School of Built Environment, Engineering and Computing, Leeds Beckett University, Leeds, LS2 8AJ, UK
[2]School of Engineering, Cardiff University, Cardiff, CF24 3AA, UK
[*]Author for correspondence: Dr Nikolay Perepelkin, N.Perepelkin@leedsbeckett.ac.uk

Abstract

The classic Johnson-Kendall-Roberts (JKR) contact theory was developed for frictionless adhesive contact between two isotropic elastic spheres. The advantage of the classical JKR formalism is the use of the principle of superposition of solutions to non-adhesive axisymmetric contact problems. In the recent years, the JKR formalism has been extended to other cases, including problems of contact between an arbitrary shaped blunt axisymmetric indenter and a linear elastic half-space obeying rotational symmetry of its elastic properties. Here the most general form of the JKR formalism using the minimal number of a priori conditions is studied. The corresponding condition of energy balance is developed. For the axisymmetric case and a convex indenter, the condition is reduced to a set of expressions allowing explicit transformation of force-displacement curves from non-adhesive to corresponding adhesive cases. The implementation of the developed theory is demonstrated by presentation of a two term asymptotic adhesive solution of the contact between a thin elastic layer and a rigid punch of arbitrary axisymmetric shape. Some aspects of numerical implementation of the theory by means of Finite Element Method are also discussed.

Keywords: adhesion, the JKR theory, axisymmetric contact, parametric force-displacement curve, Finite Element Method

1 Introduction

The classic formulation of the Hertz-type contact problems was independently introduced by Hertz (1882) and Boussinesq (1885) (see references in [1]). This formulation of Hertz contact theory assumes that the shape of the bodies and the compressing force P are given and molecular adhesion can be ignored. Hence, the displacements and stresses appear in the solids only after the external load is applied. In addition, it is assumed that the contact region is small in comparison with the characteristic size of contacting solids and, therefore, the boundary value problem for the solids may be formulated as a boundary value problem for an isotropic elastic half-space. A particular case of the Hertz solution can be used for a spherical punch that is approximated as a paraboloid of revolution. In the framework of the Hertz contact theory for axisymmetric punches, several authors found relations between the radius of the contact region a, the force P and the approach between solids δ for punches whose shape functions f are monomial $f(r) = B_d r^d$, where r is the polar radius, d is the degree of the monom, and B_d is a positive constant whose physical dimension depends on d. In particular, Love [2] obtained a solution for $d = 1$ (a cone), Shtaerman [3] presented a solution for $d = 2n$ where n is an arbitrary natural number, and Galin [4] solved the problem for an arbitrary $d > 1$. In fact Galin [4, 5] presented a solution for an arbitrary convex punch of revolution.

It is important to note that the influence of effects of adhesion between solids increases at micro-/nanometer length scales. Assuming that adhesion between points of two rigid spheres of radii R_1 and R_2 respectively, is caused by the London intermolecular forces and that these interactions are additive, Bradley [6] calculated the force of adhesion P_{adh} between the spheres as $P_{adh} = 2\pi w R$ where R is the effective radius of the spheres $R^{-1} = R_1^{-1} + R_2^{-1}$, and w is the work of adhesion. In fact, he calculated the force of adhesion between each point of the former sphere with all points of the later sphere and then integrated the results obtained for all points of the former sphere. The calculations were rather lengthy, while the same result was derived just in a couple of lines by Derjaguin [7] using his approximation.

Derjaguin [7] stated that elastic deformations of spheres should be taken into account in order to consider their adhesive contact. In his excellent paper Derjaguin argued that adhesive interactions may be reduced to interactions among surface elements of spheres (see a discussion about the Derjaguin approximation in [1]).

Derjaguin stated also [7] that the virtual work done by the external load during adhesive contact is equal to the sum of the virtual change of the potential elastic energy and the virtual work that is consumed by the increase of the surface attractions. Unfortunately, the paper contains some erroneous assumptions and miscalculations. Nevertheless, using Derjaguin's results, Sperling in his PhD thesis [8] derived the force-displacement diagram for a sticky sphere and analyzed the critical points of the curve. Sperling was not aware about Johnson's [9] suggestion to use the stress superposition to estimate the influence of adhesive forces. Like Derjaguin's paper, Johnson's paper was brilliant but containing a wrong statement that the adhesive interactions should be neglected. Independently of Sperling, Johnson *et al.* [10] presented the JKR (Johnson, Kendall and Roberts) theory that united Derjauguin energy approach and Johnson idea of stress fields superposition (see a discussion by Kendall [11]). In fact, it was shown that a solution to the adhesive contact problem may be derived using superposition of two non-adhesive frictionless contact problems: the Hertz solution for contact between elastic spheres and the Boussinesq solution for a flat-ended cylindrical punch. This approach to adhesive contact problems will be referred further as the JKR formalism. Due to its simplicity and elegance, the JKR approach is very popular and it has been referenced in the literature thousands of times [12].

The JKR formalism was employed to solve problems of adhesive contact between power-law shaped solids independently by Galanov [13] (see also Galanov and Grigoriev [14]) for an arbitrary $d \geq 1$ and Carpick *et al.* [15] for $d = 2n$ (see a discussion by Borodich [5]). Later Borodich and his co-workers extended the JKR formalism to arbitrary blunt axisymmetric indenters and to materials having rotational symmetry like transversely isotropic or homogeneously prestressed materials [17, 16, 1]. It was shown by Borodich [1] that using the JKR formalism along with the Griffith idea of equating the derivative of the total energy to zero [18], one can obtain the JKR expressions for a convex punch of arbitrary shape. Actually, it was shown that the derivative of the total energy will produce two terms having the same absolute value and opposite signs, i.e. these two terms vanish, and a product of some expression and a derivative of the contact radius with respect to the indentation force (da/dP). The novelty of this approach was that one did not need to express the da/dP explicitly and the the expression staying in front of the derivative was in essence the JKR solution. The Borodich approach was extended to problem of probing of stretched sticky two-dimensional (2D) membranes [19], and to problems of adhesive contact between a convex axisymmetric punch and a thin elastic layer [20] or a thin bi-layer [21] in the leading term approximation.

A major development occurred in works by Shull and his collaborators [22, 23]. Using a method called "the compliance method", they derived formulae linking energy release rate, the values of contact force and displacement related to the same contact area on force-displacement curves in a non-adhesive case and the corresponding JKR adhesive one. Nonetheless, Shull's works did not suggest to use those formulae to reduce solutions of contact problems from one case to the other.

Recently a further improvement to the JKR theory was suggested in the works by Popov and his collaborators [24, 25]. Similarly to Borodich [1], it was shown that the derivative of the total energy of an adhesive contact produces two terms that vanish and a product of some expression that is a JKR-type solution and a derivative of the contact radius with respect to the indentation force; and similarly to Shull's work [22], yet using a different mathematical justification, they were able to develop formulae that allowed explicit transformation from the solutions to largely arbitrary axisymmetric non-adhesive contact problems to the JKR-type solutions of the adhesive problems. In fact, those formulae made redundant a number of semi-analytical models of adhesive contact, for instance, Finite Element Method-based approaches [26, 27, 28] developed to describe adhesive contact between a rigid indenter and an elastic layer of finite thickness by means of introducing correction factors into the classical JKR relations for elastic half-spaces.

The above mentioned approach [24, 25] contains *a priori* assumptions, such as constant contact stiffness during the virtual "unloading" stage. Those assumption are required to reach the true configuration of the system in the JKR approach. In contrast, here the same problems are studied without employment of any assumptions concerning the mathematical form of the involved force-displacement relations, assuming only the validity of the JKR formalism, i.e. the validity of the superposition principle of the contact problems for axial symmetric problems. See Section 2(a) for details of representation of the JKR formalism as a virtual two-stage "loading-unloading" process. As a consequence, additional mathematical conditions arise naturally, as we employ the original approach presented in the classical paper [10] and derive a general form of the energy balance condition of the JKR theory without specifying a particular form of the indentation force-displacement relations (Section 2(b)). Those extra conditions, leading to the explicit formulae of the JKR formalism, and their validity scope are considered in Section 3. Further, the implementation of the developed theory is demonstrated by presenting a two term asymptotic adhesive solution of the contact between a thin elastic layer and a rigid punch of arbitrary axisymmetric shape (Section 4). Section 5 contains discussion concerning some limitations of the presented theory and certain aspects of its practical implementation by means of Finite Element Method. In particular, it has been shown that the complete set of values required for practical use of the explicit JKR formulae (these connect the force, displacement, contact radius, slope, and the first derivative of slope) can all be accurately evaluated from FEM results by means of combined use of the original convex punch model along with a set of auxiliary flat-ended punch problems (the two-model approach).

2 Energy balance and the explicit form of the JKR formalism

It will be shown here that an adhesive contact problem can be reduced to non-adhesive ones using the classical JKR formalism. All steps of the JKR energy balance are done in the most general form producing expressions that can be used for explicit converting of the solutions to the problems.

First, consider a reference non-adhesive contact problem for an elastic medium (half-space, multilayered half-space, a single layer etc.) and an axisymmetric convex rigid punch described in the polar coordinates (r, φ, z) by the function $z = f(r)$ (the Hertz-type problem, Fig. 1,a). It is supposed that the elastic medium obeys the principle of superposition of loads. Only vertical displacements of the punch are allowed. Denoting the amount of applied force as P, the punch displacement as δ, and the radius of the contact area as a, one can formulate the solution of the Hertz-type problem in one of the two alternative parametric forms:

$$\begin{cases} P = P_H(a), \\ \delta = \delta_H(a). \end{cases} \qquad \begin{cases} \delta = \widehat{\delta}_H(P), \\ a = a_H(P). \end{cases} \tag{1}$$

Here a_H is the inverse of the P_H function, and $\widehat{\delta}_H(P) = \delta_H(a_H(P))$. In addition, under the same assumptions we consider an *auxiliary* contact problem for a circular cylindrical flat-ended punch and the same elastic medum (the Boussinesq-type problem, Fig. 1,b). The punch radius is supposed to be *exactly* the same as in the Hertz-type problem above and is also denoted as a. Let the solution of the auxiliary problem be

$$\delta = \delta_B(a, P) \tag{2}$$

The presence of the punch radius a as the parameter in the latter relation is explicitly emphasized. Both relations (1) and (2) are supposed to be known ones.

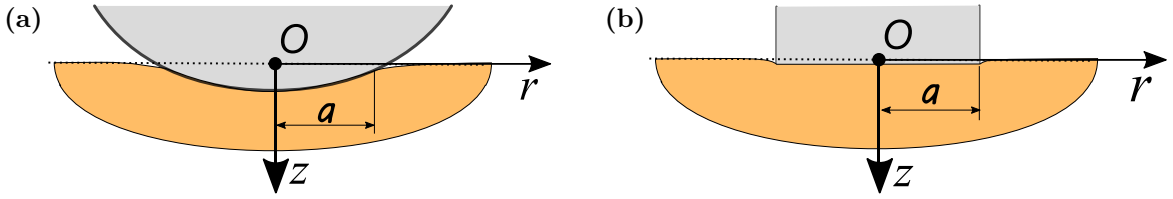

Figure 1: (a) The reference Hertz-type contact problem for a convex axisymmetrical punch; (b) The auxiliary Boussinesq-type contact problem for a cylindrical flat-ended punch.

2.1 The classical JKR formalism

The classical JKR formalism [10] suggests that the adhesive solution for the reference contact problem can be constructed as the result of a two-stage imaginary loading-unloading experiment (Fig. 2,a). The true configuration of the contact problem with adhesion can be reached in the following way (arrows in Fig. 2,a). First, the forces of adhesion are not taken into account. Therefore, under the true value of the applied force $P = P_0$ the contact area is smaller than it is in adhesive case, and the radius of the contact area $a = a_0$ is smaller than the true one (Fig. 2).

To obtain the true configuration of the contact area, the punch load is increased to the value $P = P_1$ such that the radius of the contact area $a = a_1$ becomes exactly the same as it would be in adhesive case under true load P_0. However, the applied value of force is now greater than the true one, and hence the punch displacement $\delta = \delta_1$ is not the true one. The following relation are true: $P_1 = P_H(a_1)$, $\delta_1 = \delta_H(a_1)$ and $\delta_1 = \widehat{\delta}_H(P_1)$, $a_1 = a_H(P_1)$.

On the second stage of the imaginary process, adhesive forces are "applied", that is, "turned on" within the contact region, and the punch is *unloaded back* to the true value of force P_0 while maintaining the radius of the contact area unchanged (the true one $a = a_1$). The punch displacement becomes $\delta = \delta_2$, which is the correct one for the adhesive contact problem. Thus, in the end of unloading stage the force value $P = P_0$, the displacement value $\delta = \delta_2$, and the contact radius value $a = a_1$ all become the true ones for the adhesive contact problem which means that the true configuration is reached. The above subscript notation P_0, a_1, δ_2 follows the classical work by Johnson *et al.* [10].

Since the superposition principle is supposed to be valid, the unloading stage can be considered as the result of superposition of the flat punch solution corresponding to the true contact radius a_1, and the solution of the Hertz-type problem at the point $P = P_1$. Hence, the unloading path in the $P - \delta$ coordinates can be considered a part of the force-displacement curve of the Boussinesq-type problem $\delta = \delta_B(a, P)$ at $a = a_1$ between the force values P_0 and P_1 translated to the point of the loading (Hertz) curve at which the force reaches the value $P = P_1$ (bold line in Fig. 2,b, translation of the flat punch force-displacement curve is denoted by arrows).

Introducing notation $\delta_{1B} = \delta_B(a_1, P_1)$ and recalling that $\delta_1 = \widehat{\delta}_H(P_1)$ one obtains that the unloading part of the loading-unloading path in the $P - \delta$ coordinates can be mathematically expressed as

$$\delta = \delta_{unload}(a_1, P_1, P) = \delta_B(a_1, P) + (\delta_1 - \delta_{1B}) = \delta_B(a_1, P) + \widehat{\delta}_H(P_1) - \delta_B(a_1, P_1) \tag{3}$$

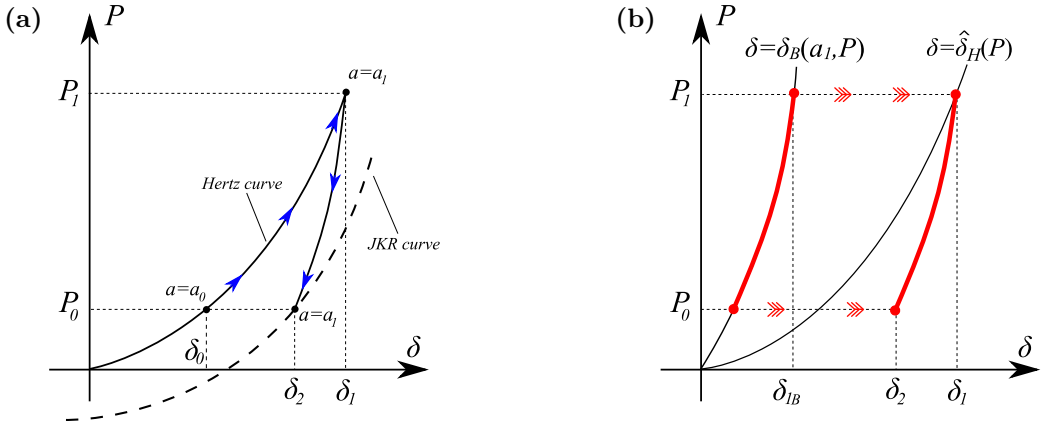

Figure 2: (a) Construction of the JKR adhesive force-displacement curve as the result of imaginary loading-unloading process (the loading-unloading path marked with arrows); (b) Superposition of the flat punch solution (the Boussinesq-type problem) during the process of construction of the JKR force-displacement curve.

where a_1 and P_1 act as parameters. In contrast, δ and P are considered variables here.

The above classical JKR approach employs the Griffith idea [18] that derivative of the total energy of the system U_T, is zero in the true configuration, i.e.

$$\frac{dU_T}{da_1} = 0, \qquad \frac{dU_T}{dP_1} = 0. \tag{4}$$

2.2 Explicit formulae of the JKR theory

Consider the total energy U_T of the system "punch-elastic medium" with adhesion. The total energy can be built up of the stored elastic energy U_E, the mechanical energy in the applied load U_M and the surface energy U_S. In turn, the elastic energy U_E can be expressed as the difference between the stored elastic energies corresponding to the loading (U_{E1}) and unloading (U_{E2}) parts of the loading-unloading diagram: $U_E = U_{E1} - U_{E2}$. Hence, the total energy of the system can be written as

$$U_T = U_{E1} - U_{E2} - U_M + U_S \tag{5}$$

Now consider separate graphical representation for all the positive and the negative terms in (5) using the loading-unloading diagram from Fig. 2. The term U_{E1} is the amount of the elastic energy stored during the loading process, and it can be calculated as $U_{E1} = \int_0^{\delta_1} P_H(\delta)d\delta$, where P_H is defined in (1). Graphically, U_{E1} can be represented as the area under the curve representing the solution of the Hertz-type problem (Fig. 3,a). The term U_{E2} is the amount of the elastic energy released during the unloading process. It can be calculated as $U_{E2} = \int_{\delta_1}^{\delta_2} P_{unload}(\delta)d\delta$, where $P_{unload}(\delta)$ denotes force-displacement relation during unloading that is, the inverted expression (3). Hence, U_{E2} can be graphically represented as a curvilinear trapezoid built on the unloading branch of the imaginary loading-unloading process (the strip-filled area in Fig. 3,b). The term U_M can be computed as $U_M = P_0\delta_2$ and thus can be represented as a rectangular area in Fig. 3.

Addition, in the algebraic sense, of the terms in (5) can be graphically represented as overlapping of the areas representing U_{E1}, U_{E2}, and U_M, which is depicted in Fig. 4. This overlapping shows that a number of components in the total energy cancel one another as they have the same values and the opposite signs (these are represented as the areas filled black in Fig. 4). Therefore, the total energy of the system can be reduced to just three components: U_+, U_- (depicted in Fig. 4 as the strip-filled areas), and U_S in the following way:

$$U_T = U_+ - U_- + U_S \tag{6}$$

Now return to the condition of the minimum of the total energy in the form of the second expression (4). The above considerations do not imply variation of the true force value P_0 in any way. Hence, $^{dU_-}/_{dP} \equiv 0$, and the condition (4), which defines the true configuration of the system, can be re-written as

$$\frac{dU_T}{dP_1} = \frac{dU_+}{dP_1} + \frac{dU_S}{dP_1} = 0 \tag{7}$$

Numerically, the value of U_+ is equal to the area of the corresponding area in Fig. 4. Hence, the value of U_+ can

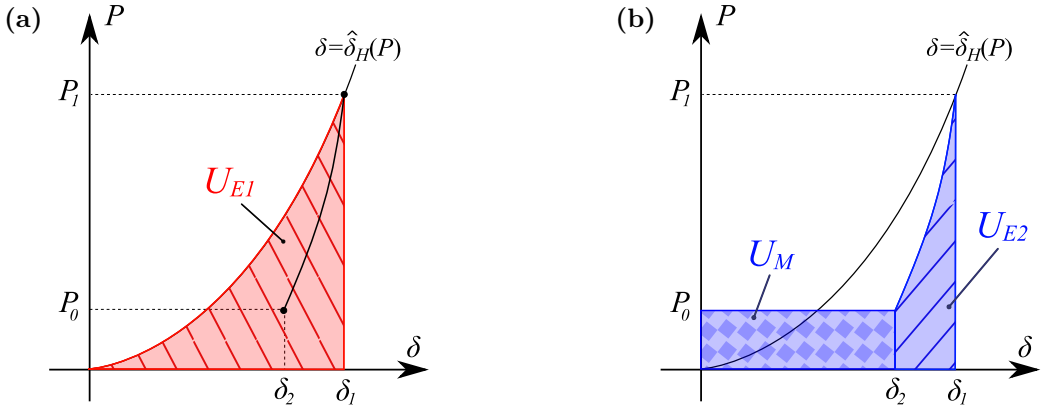

Figure 3: Representation of terms in the total energy U_T. (a) U_{E1}; (b) U_{E2} and U_M.

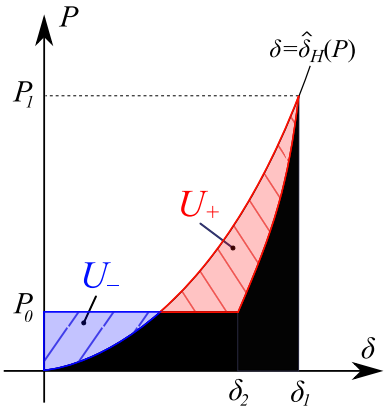

Figure 4: Graphical representation of different terms in the expression for the total energy U_T that cancel (black area) and do not cancel one another (strip-filled areas).

be calculaetd in the form of the following integral:

$$U_+ = \int_{P_0}^{P_1} \left[\delta_{unload}(a_1, P_1, P) - \widehat{\delta}_H(P)\right] dP = \int_{P_0}^{P_1} \left[\delta_B(a_1, P) + \widehat{\delta}_H(P_1) - \delta_B(a_1, P_1) - \widehat{\delta}_H(P)\right] dP \tag{8}$$

or in a simplified form

$$U_+ = (P_1 - P_0)\left[\widehat{\delta}_H(P_1) - \delta_B(a_1, P_1)\right] + \int_{P_0}^{P_1} \left[\delta_B(a_1, P) - \widehat{\delta}_H(P)\right] dP \tag{9}$$

Hence, the total derivative $^{dU_+}/_{dP_1}$ can be written after some transformations as

$$\begin{aligned} \frac{dU_+}{dP_1} = (P_1 - P_0)&\left[\frac{d\widehat{\delta}_H(P_1)}{dP_1} - \frac{\partial \delta_B(a_1, P_1)}{\partial P_1} - \frac{\partial \delta_B(a_1, P_1)}{\partial a_1}\frac{da_H(P_1)}{dP_1}\right] \\ &+ \int_{P_0}^{P_1}\left[\frac{\partial \delta_B(a_1, P)}{\partial a_1}\frac{da_H(P_1)}{dP_1}\right] dP \end{aligned} \tag{10}$$

In the latter expression we take into account that a_1 depends on P_1 as $a_1 = a_H(P_1)$. The differentiation rule applied is: if $J = \int_\alpha^x f(x,t)dt$, then $\frac{dJ}{dx} = f(x,x) + \int_\alpha^x \frac{\partial f(x,t)}{\partial x}dt$.

In axisymmetrical contact problem the surface energy U_S can be expressed as $U_S = -\pi w a_1^2$, where w is the work of adhesion which is equal to the amount of energy per unit area needed to separate two surfaces from initial contact to infinite distance. Hence

$$\frac{dU_S}{dP_1} = -2\pi w a_1 \frac{da_1}{dP_1} = -2\pi w a_1 \frac{da_H(P_1)}{dP_1} \tag{11}$$

Thus, using the above expressions the condition of the minimum of the total energy (7) in general form becomes

$$\frac{dU_T}{dP_1} = (P_1 - P_0)\left(\frac{d\widehat{\delta}_H(P_1)}{dP_1} - \frac{\partial\delta_B(a_1,P_1)}{\partial P_1}\right) + \\ + \left[\int_{P_0}^{P_1}\frac{\partial\delta_B(a_1,P)}{\partial a_1}dP - (P_1-P_0)\frac{\partial\delta_B(a_1,P_1)}{\partial a_1} - 2\pi w a_1\right]\frac{da_H(P_1)}{dP_1} = 0 \tag{12}$$

The latter expresion can be considered the most general form of the energy balance condition of the JKR theory as it has been developed without any particular assumptions regarding mathematical form of the solutions of the Hertz-type and the Boussinesq-type problems. The only assumptions implemented here are the assumption of validity of the superposition principle for the considered elastic medium, and the axial symmetry of the problem.

The above general expression can be significantly simplified under the following two assumptions (the scope of their validity will be discussed in the next Section).

Condition 1: *At any given value of the true contact radius a_1 the curves related to the Hertz-type problem and the Boussinesq-type problem have identical slopes;*

Condition 2: *The solution of the Boussinesq-type problem is linear with respect to both δ and P.*

Indeed, Condition 1 can be mathematically expressed as

$$\frac{d\widehat{\delta}_H(P_1)}{dP_1} = \frac{\partial\delta_B(a_1,P_1)}{\partial P_1} \tag{13}$$

which makes the first term in (12) exactly zero. Further, Condition 2 suggests that the solution (2) of the Boussinesq problem can be represented as

$$\delta = \frac{P}{S(a_1)} \tag{14}$$

That is, the function $\delta_B(a_1,P)$ (see (2)) is equal to $P/S(a_1)$ where $S(a_1) = dP/d\delta$ is the corresponding slope of the Boussinesq-type solution. Clearly, $\frac{\partial\delta_B(a_1,P)}{\partial a_1} = -({}^{P}/_{S^2(a_1)})({}^{dS}/_{da_1})$.

Denoting the total derivative with respect to the true value of contact radius with prime ($'$) and assuming that both Conditions 1 and 2 are true, as well as $da_H(P_1)/dP_1 \neq 0$, (12) becomes

$$\frac{(P_1-P_0)^2}{2}\frac{S'(a_1)}{S^2(a_1)} = 2\pi w a_1 \tag{15}$$

The latter expression readily gives the amount of unloading $P_1 - P_0$ necessary for the transformation from the non-adhesive solution of the Hertz-type problem to the JKR adhesive one. In fact, $P_1 - P_0$ is the additional term that has to be subtracted from the expression for the contact force in order to reduce the non-adhesive problem to the adhesive one:

$$P_1 - P_0 = \sqrt{\frac{4\pi w a_1 S^2(a_1)}{S'(a_1)}} \tag{16}$$

Since the unloading curve is now supposed to be linear, according to (14), the increment of punch displacement $\delta_1 - \delta_2$ obeys the following law: ${}^{(P_1-P_0)}/_{(\delta_1-\delta_2)} = S(a_1)$. Therefore, (16) leads to

$$\delta_1 - \delta_2 = \sqrt{\frac{4\pi w a_1}{S'(a_1)}} \tag{17}$$

Note that the values P_1, δ_1, a_1 always correspond to a point on the Hertzian non-adhesive curve because $P_1 = P_H(a_1)$, $\delta_1 = \delta_H(a_1)$. In the light of (16) and (17), the solution of the corresponding JKR adhesive problem can be now written as

$$P_H(a_1) - P_0 = \sqrt{\frac{4\pi w a_1 S^2(a_1)}{S'(a_1)}}, \qquad \delta_H(a_1) - \delta_2 = \sqrt{\frac{4\pi w a_1}{S'(a_1)}} \tag{18}$$

Further we remove auxiliary subscripts and will use the notations P, δ and a instead of P_0, δ_2 and $a_1$for the true values of the total force, the punch displacement and the contact radius in the adhesive contact problem. Thus, the following formulae can be used to reduce the solution of an adhesive-less axisymmetric contact problem into the corresponding solution of the JKR adhesive contact problem:

$$P = P_H(a) - \sqrt{\frac{4\pi w a S^2(a)}{S'(a)}}, \qquad \delta = \delta_H(a) - \sqrt{\frac{4\pi w a}{S'(a)}} \tag{19}$$

where

$$S(a) = \frac{dP_H}{d\delta_H} = \frac{P'_H(a)}{\delta'_H(a)} \tag{20}$$

is the slope of the non-adhesive $P-\delta$ curve which is supposed to be identical to the slope of the auxiliary Boussinesq-type problem according to (13).

The formulae (19) allow to reduce an arbitrary axisymmetric non-adhesive contact problem to the JKR-type adhesive one explicitly, without the need to develop and solve the equations of energy balance.

It is interesting to note that particular cases of the expressions (19) were discussed by Shull et al. [22] (see the expressions (11) and (12) in their paper), however the formulae were not applied to extend the JKR theory for arbitrary shaped solids and they were not suggested as means of explicit transformation between non-adhesive and adhesive solutions. As it has been mentioned above, the JKR theory was extended to the power-law shapes of indenters independently by Galanov [13] (for arbitrary exponents of the power-law) and by Carpick et al. [15] (for integer exponents of the power-law). For arbitrary axisymmetric shape of the indenter, this generalization was presented by Borodich [1] still using the Hertzian half-space approximation of the contacting medium. The difference between the approaches to a power-law shaped indenter and an arbitrary shaped indenter was that the $P-\delta$ relations for power-law shaped indenters may be presented explicitly (see Galin [4], while Borodich did not write these expressions but instead he employed the formulae for $dP/d\delta$ in his calculations of the derivative of the total energy. The latter approach can be expressed using the formulae (19) as it was eventually shown by Popov [24] and Argatov *et al* [25].

In the next Section, the scope of Conditions 1 and 2, used to develop the above explicit JKR formulae, is investigated for some general cases.

3 Some properties of the slopes of the Hertz-type and Boussinesq-type force-displacement curves

In the previous Section, two statements, related to the properties of the slopes of the Hertz-type and Boussinesq-type force-displacement curves, were used to simplify the general condition of the minimum of the total system energy (12) into the explicit form of the JKR theory (19). Here the scope of these statements is discussed and proven for some particular cases.

The validity of those two properties, the linearity of the solution of Boussinesq-type problem, and the equality of the slopes of a Boussinesq-type problem and the respective Hertz-type problem at the same contact radius, can be proven relatively easily when well-known solutions of classical problems of Contact Mechanics are considered. For instance, the below short analytical examples demonstrate validity of the two properties (13)-(14).

1) *Elastic isotropic half-space, rigid smooth convex axisymmetric indenter of arbitrary shape.*

Consider the solution of the frictionless contact problem for an axisymmetric smooth indenter of arbitrary shape defined in cylindrical coordinates by the function $z=f(r)$, and an elastic isotropic half-space. Here we use the solution in the form developed by Galin (see discussion and references in [1]):

$$P_H = 2E^* \int\limits_0^a r\Delta f(r)\sqrt{a^2-r^2}dr, \qquad \delta_H = \int\limits_0^a r\Delta f(r)\text{arctanh}\left(\sqrt{1-\frac{r^2}{a^2}}\right)dr. \tag{21}$$

An alternative form of the above relations was developed by Rostovtsev [29] and Sneddon [30]. The detailed transformation between the two solutions is also discussed in [1].

Having performed differentiation of the above expressions, one can obtain after some transformations the slope of the $P-\delta$ curve (21) as

$$S_H(a) = \frac{dP_H}{d\delta_H} = \frac{dP_H/da}{d\delta_H/da} = 2E^*a. \tag{22}$$

The force-displacement relation of the contact problem for a cylindrical indenter of radius a and the same elastic half-space, and the corresponding slope are

$$P_B = 2E^*a\delta_B, \qquad S_B(a) = \frac{dP_B}{d\delta_B} = 2E^*a, \tag{23}$$

which readily confirms the properties of slopes (13)-(14) for this case. In the above expressions, E^* denotes the effective elastic modulus of the half-space: $E^*=E/(1-\nu^2)$ where the Young modulus and Poisson's ratio of the half-space are denoted as E, ν.

2) *Elastic transversely isotropic half-space, rigid smooth axisymmetrical indenter.*

It is known [31, 32], that a transversely isotropic elastic half-space has the same surface influence function (the Green function), as an isotropic elastic half-space, except that the elastic modulus E^* in the latter case is substituted with a different elastic modulus E_{TI} in the former case. The modulus E_{TI} depends on the five independent elastic moduli that form the tensor of elastic constants of the transversely-isotropic material. Thus, having substituted E^* with E_{TI} in the above equations, one can readily prove correctness of properties (13)-(14).

In more complex cases, e.g. layers of finite thickness, multilayered medium, the validity of the formulae (13)-(14) may be less obvious, as simple analytical solutions are not always readily available. Hence, in the remaining part of the present Section we provide proofs of the formulae (13)-(14) for more general cases. We again consider the two non-adhesive contact problems introduced in the previous Section: the Hertz-type problem for a convex

axisymmetric rigid punch, and the Boussinesq-type problem for a flat-ended punch of the same radius a. The shape of the convex punch is defined in the cylindrical coordinates (r, φ, z) by the function $z = f(r)$.

First, we present a proof of the linearity of the force-displacement dependency for the Boussinesq-type problem under the following assumptions.

Consider a contact problem for a rigid flat-ended punch with cylindrical side surface (the Boussinesq-type problem, Fig. 5,a) and an elastic medium (half-space, multilayered half-space, a single layer etc.) Assume that the elastic medium obeys the principle of the superposition of loads, the flat side of the punch is in full contact with it, and the contact problem is frictionless. Let P be the external force applied to the punch and acting alongside its generating line, punch movement in all other directions is prohibited. The punch penetration is denoted δ.

In that case, the force-displacement dependency for the problem can be represented in the form $P = \delta S_B$, which is linear with respect to P and δ. The quantity S_B depends on the geometric parameters of the punch base, and not on the penetration depth. If the punch base is a circle of radius a, then S_B is a function of a, and the force-displacement dependency for the problem has form $P = \delta S_B(a)$.

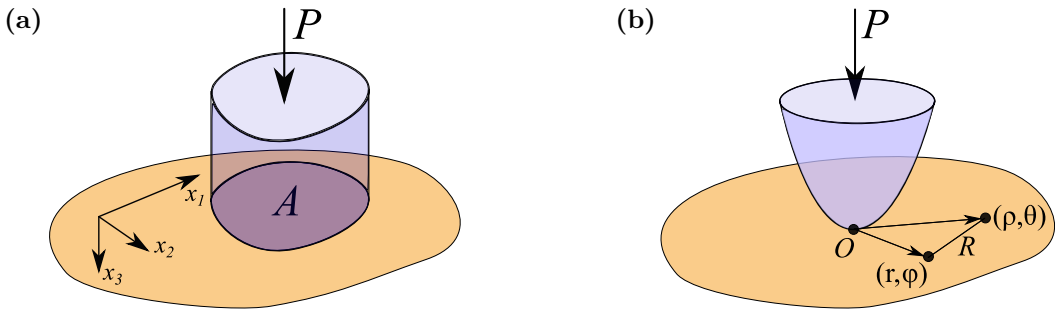

Figure 5: (a) Contact problem for an arbitrary flat-ended punch with cylindrical side surface; (b) Contact problem for an arbitrary axisymmetrical smooth convex punch.

Proof. Consider the main contact problem, which has punch penetration equal to δ and normal pressure distribution denoted as $p(x_1, x_2)$, and an auxiliary one, which has punch penetration equal to 1 and normal pressure distribution denoted as $p^*(x_1, x_2)$, where x_1, x_2 are the spatial coordinates associated with the contact area (Fig. 5,a). The contact problems are both assumed frictionless, hence only normal contact pressure acts within the contact area A, which does not change at any load.

Since the elastic medium obeys the principle of superposition of loads, both problems can be expressed in the form of integral equations:

$$\iint\limits_A p^*(\xi_1, \xi_2) K(R) d\xi_1 d\xi_2 = 1, \qquad \iint\limits_A p(\xi_1, \xi_2) K(R) d\xi_1 d\xi_2 = \delta. \tag{24}$$

Here $K(R)$ is the convolution kernel, the surface influence function of the elastic medium, and $R = \sqrt{(\xi_1 - x_1)^2 + (\xi_2 - x_2)^2}$ is the distance between the current point (ξ_1, ξ_2) and some selected point (x_1, x_2) on the surface.

Apart from the elastic constants of the elastic medium, which are a part of the kernel $K(R)$, the pressure distribution p^* implicitly depends on geometrical parameters of the contact area A, as this is the integration domain in (24). Due to linearity of the double integral, it is clear that pressure distribution p, which is the solution of the second equation (24), can be expressed as:

$$p(\xi_1, \xi_2) = \delta\, p^*(\xi_1, \xi_2). \tag{25}$$

Finally, the total force P applied to the punch can be calculated as

$$P = \iint\limits_A p(x_1, x_2) dx_1 dx_2 = \delta \iint\limits_A p^*(x_1, x_2) dx_1 dx_2 = \delta S_B \tag{26}$$

where $S_B = \iint\limits_A p^*(x_1, x_2) dx_1 dx_2$ does not depend on δ, and depends only on material properties and geometrical parameters of the contact area. If the contact area is a circle with radius a, then $S_B = S_B(a)$, as a becomes an integration limit in (26) and (24) if these expressions are reduced to polar coordinates.

Apparently, this proof mostly follows from the assumed validity of the superposition principle, which readily leads to the linear integral equations (24). Hence, one may expect similar slope properties in more advanced cases, like contact with friction.

Note that the expresion S_B represents the total force value required to produce the unit displacement of the considered cylindrical punch.

Next, we present a proof of the equality of the slopes of a Boussinesq-type problem and Hertz-type problem at the same contact radius using assumption as follows.

*Consider a convex axisymmetrical punch pressed against an elastic medium (half-space, multilayered half-space, a single layer etc.) with the force P (normal contact) and assume the contact problem to be frictionless (the Hertz-type problem) with contact pressure greater than zero inside the contact area and equal to zero on its edge. Let δ be the punch penetration. If the elastic medium obeys the principle of the superposition of loads and has circular symmetry of elastic properties (i.e. isotropic, transversely isotropic) around the direction of punch action, then for any non-zero value of the radius of the contact area a the slope $S = dP/d\delta$ of the load-displacement curve $P(\delta)$: **(i)** does not depend explicitly on the indenter shape but rather on the radius a of the contact area; **(ii)** has the same value as the slope of the contact problem for the same medium and a flat-ended cylindrical punch of radius a (the Boussinesq-type problem).*

Proof. Because both the elastic medium and the convex punch are axisymmetric, the contact area A in the normal contact is a circle of radius a. Both the total force P and the punch displacement δ can be expressed as functions $P = P(a), \delta = \delta(a)$.

The whole problem can be reduced to cylindrical coordinates. Let r be the polar radius, φ be the polar angle, and the point O of initial contact be the coordinate origin (Fig. 5,b). Denote $f(r)$ the punch shape function in cylindrical coordinates.

The contact problem is assumed frictionless, hence only normal contact pressure arise within the contact area A. Due to the axial symmetry of the problem, normal contact pressure distribution is axisymmetric too and can be expressed by an unknown function $p(a, r)$. Here we explicitly emphasize that particular stress distribution depends on the value of the contact radius as a parameter, which is linked to P and δ as described above.

Consider the governing integral equation of the contact problem:

$$\iint\limits_A p(a,\rho)K(R)dA = \delta(a) - f(r) \tag{27}$$

Here $K(R)$ is the surface influence function of the elastic medium, and R is the distance between the current point (ρ, θ) and some selected point (r, φ) on the surface (Fig. 5,b). Here (ρ, θ) are dummy coordinates used as integration variables in (27). In polar coordinates, the distance R is expressed as $R = \sqrt{r^2 + \rho^2 - 2r\rho\cos\varphi\cos\theta - 2r\rho\sin\varphi\sin\theta}$. Since the reference for both angular coordinates, φ and θ, can always be chosen in such a way that $\varphi = 0$, the latter expression can be reduced to the following form without loosing generality: $R = \sqrt{r^2 + \rho^2 - 2r\rho\cos\theta}$.

Hence, the integral equation (27) can be now written in the following form:

$$\int\limits_0^a p(a,\rho)\mathcal{L}(r,\rho)d\rho = \delta(a) - f(r), \tag{28}$$

where $\mathcal{L}(r,\rho) = \rho \int\limits_0^{2\pi} K(\sqrt{r^2 + \rho^2 - 2r\rho\cos\theta})d\theta$.

Eq. (28) can be differentiated with respect to a, which yields

$$\frac{d\delta(a)}{da} = \left[p(a,a)\mathcal{L}(r,a) + \int\limits_0^a \frac{\partial p(a,\rho)}{\partial a}\mathcal{L}(r,\rho)d\rho\right] \tag{29}$$

Because $p(a, a) \equiv 0$ the formula (29) becomes:

$$\frac{d\delta(a)}{da} = \int\limits_0^a \frac{\partial p(a,\rho)}{\partial a}\mathcal{L}(r,\rho)d\rho \tag{30}$$

This is an integral equation with respect to the unknown function $\dfrac{\partial p(a,r)}{\partial a}$. Since the equation is linear, one can always represent its solution as

$$\frac{\partial p(a,r)}{\partial a} = \frac{d\delta(a)}{da}\,\psi^*(a,r) \tag{31}$$

where $\psi^*(a, r)$ is the is the solution of the auxiliary equation:

$$\int\limits_0^a \psi^*(a,r)\mathcal{L}(r,\rho)d\rho = 1 \tag{32}$$

The solution of the auxiliary equation, function $\psi^*(a, r)$, depends explicitly on the radius a, and does not depend on the punch shape. There is no explicit dependency on either punch penetration, or the total force.

Now consider the total applied force, which can be evaluated in cylindrical coordinates as the integral of the contact pressure $p(a, r)$:

$$P(a) = 2\pi \int\limits_0^a p(a,r)r dr \tag{33}$$

The total derivative of P with respect to a becomes

$$\frac{dP(a)}{da} = 2\pi \left[ap(a,a) + \int_0^a \frac{\partial p(a,r)}{\partial a} r dr \right] \tag{34}$$

Since the contact pressure on the boundary of the contact area is supposed to be zero $p(a,a) \equiv 0$, the latter is simplified to

$$\frac{dP(a)}{da} = 2\pi \int_0^a \frac{\partial p(a,r)}{\partial a} r dr \tag{35}$$

Finally, (31) can be substituted into (35) which yields

$$\frac{dP}{da} = 2\pi \int_0^a \frac{\partial p(a,r)}{\partial a} r dr = 2\pi \frac{d\delta}{da} \int_0^a \psi^*(a,r) r dr \tag{36}$$

The latter allows one to find the slope of the force-displacement curve:

$$S = \frac{dP}{d\delta} = \frac{dP(a)/da}{d\delta(a)/da} = 2\pi \int_0^a \psi^*(a,r) r dr \tag{37}$$

which is a function of the contact radius a. Thus, the slope value does not depend explicitly on the indenter shape, because $\psi^*(a,r)$ depends explicitly only on the radius a.

Now consider the same contact problem formulated for cylindrical punch of the same radius as the current contact radius a (the Boussinesq-type problem). Denote p_B the distribution of the contact pressure for this problem. Having repeated the transformations (27)-(28), one can write the governing integral equation for the Boussinesq-type problem in cylindrical coordinates as

$$\int_0^a p_B(a,\rho) \mathcal{L}(r,\rho) d\rho = \delta \tag{38}$$

where a is a constant parameter, and an auxiliary integral equation that corresponds to the contact problem with unity punch displacement:

$$\int_0^a p_B^*(a,\rho) \mathcal{L}(r,\rho) d\rho = 1 \tag{39}$$

It follows from the proof above, that the slope of the Boussinesq-type force-displacement curve S_B is equal to the total force required to produce the unit displacement of the considered cylindrical punch, that is

$$S_B = 2\pi \int_0^a p_B^*(a,r) r dr \tag{40}$$

Now compare expressions (39), (40), that define the slope of the Boussinesq-type force-displacement curve, and Eq. (32), (37), which define the slope of the Hertz-type force-displacement curve. It is clear that these equations are identical apart from the used notation. Since the contact radius a is supposed to be identical in both cases, both slopes are identical too.

Remark. Clearly, the above proofs are not universal and do not cover certain contact scenarios, like contact with friction (see a discussion in [1]), or some exotic cases like axisymmetric contact between a paraboloidal indenter and a circular Kirchhoff plate [33], which leads to zero contact pressure in the inner points of the contact area. Those cases are not covered in this paper and require separate consideration. Nonetheless, the above proofs cover many important situations, like contact problems for layers of finite thickness, or multi-layered medium, or Finite Element Method-based models of finite size. Section 5 contains a description of a two-model finite elements-based approach to the construction of parametric force-displacement curves that is heavily based on the above properties of slopes.

Although some of the above statements might already exist in the literature (see e.g. transformations in [46, 47]), we believe that the reader would benefit from the accurate formulations of the statements and presentation their proofs consolidated in the present Section. To the best of our knowledge, there is no publication presenting in full the above statements on properties of the slopes of the $P - \delta$ curves.

4 Adhesive contact problem for a thin elastic layer: Leading term and two term asymptotic solutions

Here the explicit transformation (19) is demonstrated for asymptotic JKR adhesive contact between a rigid punch and a thin elastic layer. The cases of the leading term and two term asymptotic solutions are considered.

Consider a non-adhesive (Hertz-type) contact problem for an elastic layer of constant thickness h bonded to a rigid substrate, and an axisymmetric rigid indenter, as shown in Fig. 6. In this section we demonstrate how one can reduce a known asymptotic solution of this contact problem into the JKR adhesive one, using the previously developed formulae.

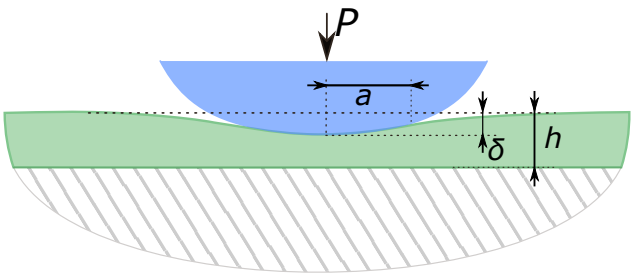

Figure 6: Contact problem for a thin elastic layer and a rigid indenter

Let P be the total force applied to the indenter, δ be the penetration depth, a be the radius of the contact area, and $f(r)$ be the function describing the shape of the indenter in the cylindrical coordinates. Assume that the layer thickness h is much smaller than the radius of the contact area a. In this case, the ratio h/a becomes a small parameter, which allows one to use asymptotic techniques to solve the contact problem. It is known (e.g. [34]) that isotropic or transversely isotropic asymptotically thin elastic layer can be reduced to the Winkler-Fuss elastic foundation in the leading term asymptotic approximation, or the Pasternak elastic foundation in the two-term asymptotic approximation. The Winkler-Fuss foundation [35] is a model that can be represented as a layer of independent springs that act in such a way that normal external pressure at some point $p(x_1, x_2)$ causes the displacement $w(x_1, x_2)$ proportional to the applied pressure: $p(x_1, x_2) = Kw(x_1, x_2)$, where K is the elastic modulus of the foundation. There are more advanced models where the external pressure p and the corresponding displacements w are linked via the following relation: $p\left(x_1, x_2\right) = Kw\left(x_1, x_2\right) - G\nabla^2 w\left(x_1, x_2\right)$, where K and G are elastic moduli of the foundation. These two elastic moduli elastic foundation models include the Pasternak foundation [36], which can be represented as a layer of springs that have shear interaction between them; and Filonenko-Borodich foundation [37], which can be represented as springs of a Winkler-Fuss fondation covered by a stretched membrane.

A contact problem for a thin isotropic layer of thickness h, with Young's modulus E and Poisson ratio ν, is considered in the book [34], which suggests the values of the elastic moduli K and G as $K = E\left(1-\nu\right)/[h\left(1+\nu\right)\left(1-2\nu\right)]$ and $G = hE\nu(1-4\nu)/[3(1+\nu)(1-2\nu)^2]$.

4.1 Leading term asymptotic adhesive solution

For the sake of completeness, first we briefly demonstrate the derivation of the leading term adhesive solution to the contact problem for an asymptotically thin elastic layer. This problem has been discussed a number of times in the literature (see e.g. review in [20]).

The total applied force P and the penetration depth δ of the Hertz-type problem in the leading term asymptotic approximation can be represented as [20]:

$$\delta_H(a) = f\left(a\right), \qquad P_H(a) = \pi K\left[a^2 f\left(a\right) - 2\int_0^a f\left(r\right) r dr\right]. \tag{41}$$

The slope of the Hertz-type curve and its derivative are therefore $S\left(a\right) = {}^{dP_H}/_{d\delta_H} = \pi K a^2$, $S'\left(a\right) = 2\pi K a$. Thus, the explicit formulae (19) can be readily written as:

$$\delta(a) = f\left(a\right) - \sqrt{\frac{2w}{K}}, \qquad P(a) = \pi K\left[a^2 f\left(a\right) - 2\int_0^a f\left(r\right) r dr - a^2\sqrt{\frac{2w}{K}}\right], \tag{42}$$

which is exactly the result derived in [20] using the classical JKR methodology [10].

4.2 Two term asymptotic adhesive solution

In this section, we use the above mentioned fact that in two term asymptotic approximation the thin elastic layer can be formally substituted with the Pasternak elastic foundation. Here we start from the governing relation between the applied pressure and the displacement of such a foundation, and represent the derivation of the corresponding JKR adhesive solution in full.

First, let us take into account axial symmetry of the problem, which allows to re-write the governing relation for the Pasternak foundation $p(x_1,x_2) = Kw(x_1,x_2) - G\nabla^2 w(x_1,x_2)$ as

$$p(r) = Kw(r) - G\left(\frac{d^2w}{dr^2} + \frac{1}{r}\frac{dw}{dr}\right) \tag{43}$$

here $p(r)$ and $w(r)$ are the contact pressure and the foundation displacement correspondingly.

Clearly, the boundary condition of unilateral contact with the rigid punch requires that $w(r) = \delta - f(r), r \in [0,a]$. Substituting the latter expression into (43), one has

$$p(r) = K(\delta - f(r)) + G\left(f''(r) + \frac{1}{r}f'(r)\right), \qquad r \in [0,a]. \tag{44}$$

The contact pressure in the non-adhesive problem becomes zero on the edge of the contact area $p(a) = 0$, which can be used to link the penetration depth δ to the contact radius a using (44):

$$\delta_H = \delta(a) = f(a) - \frac{G}{K}\left(f''(a) + \frac{1}{a}f'(a)\right) \tag{45}$$

To derive the relation between the total force P and the radius a, consider the total force, taking into account (44):

$$P = 2\pi\int_0^a p(r)\,rdr = 2\pi\left[K\int_0^a \delta r dr - K\int_0^a f(r)\,rdr + G\int_0^a \left(rf''(r) + f'(r)\right)dr\right]. \tag{46}$$

After simplification, using (45), we finally obtain

$$P_H = P(a) = \pi K\left[a^2 f(a) - 2\int_0^a f(r)\,rdr\right] + \pi Ga\left[2f'(a) - af''(a)\right] \tag{47}$$

To quickly evaluate the slope of the Hertz-type force-displacement curve $S(a) = dP_H/d\delta_H$, consider (46) explicitly emphasizing that the contact radius and the contact pressure depend on the penetration depth δ:

$$P = 2\pi\int_0^{a(\delta)} p(\delta,r)\,rdr. \tag{48}$$

It follows from (48) that

$$\frac{dP}{d\delta} = 2\pi\frac{d}{d\delta}\left[\int_0^{a(\delta)} p(\delta,r)\,rdr\right] = 2\pi\left[a(\delta)\,p(\delta,a(\delta))\,\frac{da(\delta)}{d\delta} + \int_0^{a(\delta)}\frac{\partial p(\delta,r)}{\partial\delta}rdr\right] \tag{49}$$

As long as $p(\delta,a) \equiv 0$ and $\partial p(\delta,r)/\partial\delta = K$, according to (44), we have $S(a) = dP/d\delta = 2\pi\int_0^a Krdr = \pi Ka^2$. That is, the slope value of the non-adhesive $P-\delta$ curve is the same for both leading term, and two term asymptotic approximations at the same value of the contact radius a. The latter conclusion readily implies that the extra terms related to adhesion remain the same in both the leading term and the two-term asymptotics, as follows from (19).

Finally, using (45), (47), we obtain

$$\delta(a) = f(a) - \frac{G}{K}\left(f''(a) + \frac{1}{a}f'(a)\right) - \sqrt{\frac{2w}{K}} \tag{50}$$

$$P(a) = \pi K\left[a^2 f(a) - 2\int_0^a f(r)\,rdr + \frac{Ga}{K}\left[2f'(a) - af''(a)\right] - a^2\sqrt{\frac{2w}{K}}\right], \tag{51}$$

the two-term asymptotic solution for the contact problem for a thin elastic layer and a rigid punch in the framework of the JKR theory of adhesive contact.

5 Discussion

It has been developed above an explicit form of solution to the general JKR-type problems (formulae (19)) without specifying any *a priori* conditions except the validity of the superposition principle and axial symmetry, therefore letting additional conditions (13)-(14) arise naturally in order to simplify the condition of the minimum of the total energy of the system. This is an important difference from the works [24, 25], where those conditions were set *a priori* but not articulated clearly. Indeed, these conditions were "blended" and presented in [24] in an implicit form by expressing the unloading stage of the JKR formalism at the constant contact radius a as $F(a) = F_{n.a.}(a) - k_{n.a.}\Delta l$, where $F(a)$ is the value of the force in the JKR solution (P_0 in this paper), $F_{n.a.}(a)$ is the corresponding force value in the initial non-adhesive problem problem (P_1 in this paper), Δl is the amount of unloading ($\delta_1 - \delta_0$ in this paper), and $k_{n.a.}$ is the contact stiffness in the non-adhesive problem, that is, the slope of the force-displacement curve ($\frac{dP_H}{d\delta_H}$ in this paper).

The expression $F(a) = F_{n.a.}(a) - k_{n.a.}\Delta l$ describes the unloading stage of the JKR formalism at the constant radius which effectively suggests that the solution of the corresponding Boussinesq-type problem is a linear relation between force and displacement. The formula is written in terms of increments from the system already pre-loaded to reach the contact radius a. Hence, this implicitly requires the validity of the superposition principle, as the solution of the flat-punch Boussinesq problem becomes superimposed with the pre-loaded system state. Finally, the presence of coefficient $k_{n.a.}$ implicitly suggests that the slopes of the Boussinesq-type problem and the Hertz-type problem are assumed equal at the same value of the contact radius.

The approach adopted in the present paper allowed us obtain all the above conditions in a clear and explicit form (13)-(14), and also lead to the general energy balance condition (12), which can be used for futher analysis of the JKR formalism in its most general form. However, there is another advantage in having the conditions (13)-(14) explicitly formulated, which is related to practical implementation of the explicit formulae (19).

The results of the previous section demonstrate practical application of the formulae (19) in analytical form. However, numerical implementation of the same approach, e.g. by means of the Finite Element Method (FEM), can face certain challenges related to the discrete nature of finite element models. Clearly, the radius of contact cannot be determined with arbitrary accuracy, as it is limited by the characteristic size of the FE mesh in the contact area. In addition, as loads are applied, contact elements switch their effective stiffness in a non-smooth manner based on the contact gap size (e.g. [38]). These factors lead to certain inaccuracies present in any parametric force-displacement relation in the form (1) obtained from FEM solution of a contact problem.

Now it is worth recalling that formulae (19) contain the derivative of the slope $S'(a)$. Hence, if values of P, δ, and a are the primary data obtained from a FE model, then evaluation of $S'(a)$ would require two consequtive differentiations, which would considerably amplify any fluctuations present in the initial data.

To avoid that undesired numerical effect, it has been also developed here an alternative two-model approach to the construction of parametric force-displacement curves (1), based on the assumption of simultaneous validity of the conditions (13)-(14), that is:

$$\frac{d\widehat{\delta}_H}{dP} = \frac{\partial \delta_B(a,P)}{\partial P} = \frac{1}{S(a)} \tag{52}$$

The two-model approach is graphically presented in Fig. 7. In this approach, the functions $S = S(a), S' = S'(a)$ are accurately constructed using a set of auxiliary Boussinesq-type problems, whereas the dependencies $\delta = \delta(a), P = P(a)$ are identified from the Hertz-type problem using only P and δ values and the formula (52), which links Hertz-type and Boussinesq-type problems together. Altogether, this leads to accurately constructed JKR force-displacement curve (19). Let us consider this approach in more detail.

To identify the complete set of values $a = a^*, \delta = \delta^*, P = P^*, S = S^*$ representing a point on the force-displacement curve for a convex punch (Hertz-type problem), we begin with an auxiliary problem for a flat-ended cylindrical punch of the same radius a^* (Boussinesq-type problem). The auxiliary problem allows us accurately identify the value of the slope S^* by fitting the force-displacement data with a straight line.

Then the force-displacement data for the actual Hertz-type problem is numerically identified as a set of pairs (P, δ). The values are fitted with a spline curve, and by means of numerical differentiation a point which corresponds to the same slope value S^* is identified. The respective values P^* and δ^* are the sought ones. Appendix A contains a numerical example demonstrating the accuracy and validity of this two-model approach (with computer scripts used in calculations attached as supplementary materials, please see the Data Accessibility section for more details).

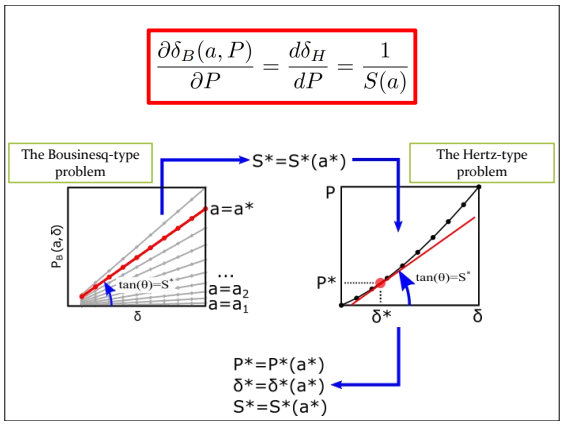

Figure 7: The two-model approach to the construction of a parametric force-displacement curve.

In this approach, the derivative $S'(a)$ can be evaluated accurately, as it would not require differentiating numerical data *two consecutive times*. Instead, a sequence of different pairs of values (a, S) from a sequence of auxiliary Boussinesq-type problems allows us construct $S'(a)$ using numerical differentiation *just once*.

We successfully implemented this concept during the development of a FEM-based equivalent of the extended Borodich-Galanov (BG) method (originally proposed in [39]) of identification of elastic properties of materials and structures by means of depth-sensing indentation [41, 40, 42]. The results have been presented at international conferences (e.g. [43]) and are being prepared for journal publication.

One more advantage of having conditions (13)-(14) explicitly stated is that the reader can better understand the validity scope of the explicit JKR formulae (19). Although those formulae seem to have been independently re-discovered in different forms by different authors [22, 23, 25, 24, 44], those works lack formal mathematical investigation of the exact applicability scope of the formulae. In this regard, the proofs developed in Section 3 can be considered an attempt to do some systematic analysis of that kind, although it is clear that those proofs do not define the entire scope and limitations of the explicit JKR formulae and more work is needed in the future. Certain limitations of the formulae (19) are highlighted in [24], such as apparent inability to reproduce in full hysteretic behaviour in force-displacement curves. At the same time, it is not entirely clear whether the formulae can be used to reproduce at least certain segments of those curves. Ciavarella [44] applied a very similar approach to investigate a contact problem of rough surfaces, although other authors [24, 45] argue that those explicit formulae should not be applied to rough contacts, at least directly. It is also worth mentioning here that in the work by Argatov et al. [25] explicit transformation from non-adhesive to the JKR adhesive solutions was done for a contact problem involving a toroidal indenter producing an annual area of contact.

6 Conclusion

The classical JKR formalism can be formulated and successfully studied in a general form employing a minimum number of a priori conditions specified, namely just axial symmetry and the validity of the superposition principle. It has been shown that the general energy balance condition can then be reduced into a set of formulae that allow solutions to non-adhesive contact problems to be explicitly transformed into the corresponding JKR adhesive solutions. For these transformations, there is no need to solve the entire problem of finding the minimum of the total potential energy of the system.

Alongside the explicit formulae of the general JKR theory, two additional mathematical conditions emerge, which can be interpreted as certain requirements imposed on the slopes of Boussinesq-type and Hertz-type force-displacement curves. The validity scope of those requirements has been discussed and formally investigated for some important practical cases. The implementation of the developed theory has been demonstrated in application to several contact problems. A problem of contact between a thin elastic layer and a rigid punch of arbitrary axisymmetric shape has been considered as an analytical example, and a two term asymptotic JKR adhesive solution has been obtained. The aspects of numerical implementation of the developed theory by means of Finite Element Method (FEM) have been discussed as well. In particular, it has been shown that the complete set of values required for practical use of the explicit JKR formulae that connect the force, displacement, contact radius, slope, and the first derivative of slope, can be accurately evaluated from FEM results by means of combined use of the original Hertz-type model along with a set of auxiliary flat-ended punch problems (the two-model approach). The advantage of the presented two-model approach is that the use of the auxiliary Boussinesq-type problems enabled us to determine accurately the slope of the $P - \delta$ curve and its derivative as functions of contact radius without differentiating numerical data two consecutive times.

Data Accessibility. The calculations presented in Appendix A can be re-created by means of Ansys

(*.apdl) and Matlab (*.m) scripts provided as supplementary materials. The scripts *Step1_problem_cyl.APDL, Step2_problem_spher.APDL, Step4_problem_spher_verification.APDL* correspond to calculation Steps 1,2, and 4 respectively. They are expected to be executed from interactive Ansys session. The script *params.apdl* contains the key calculation options and must be placed alongside the three others. The script *Step3_interpolate.m* corresponds to Step 3 and needs to be run using Matlab. Note that only the following scripts are annotated: *Step1_problem_cyl.APDL, params.apdl, Step3_interpolate.m.*

Authors' Contributions. NP and FB: the development of the generalized form of the JKR formalism (Section 2), the Discussion section (Section 5); NP: proofs in Section 3, the two-term asymptotic solution for a thin layer (Section 4(b)), initial drafting of the manuscript, all numerical computations and programming; FB: initial idea of the study, literature review (Section 1), drafting of the manuscript. All authors have read and approved the manuscript.

Competing Interests. The author(s) declare that they have no competing interests.

Funding. This work was supported by the European Union's Horizon 2020 research and innovation programme under the Marie Skłodowska-Curie grant agreement No 663830

References

[1] Borodich F.M. 2014. The Hertz-type and adhesive contact problems for depth-sensing indentation. *Advances in Applied Mechanics*, **47**, 225—366.

[2] Love A.E.H. 1939 Boussinesq's problem for a rigid cone. *Quart. J. Mathematics*, **10**, 161–175.

[3] Shtaerman I.Ya. 1939 On the Hertz theory of local deformations resulting from the pressure of elastic solids. *Dokl. Akad. Nauk SSSR*, **25**, 360–362 (Russian).

[4] Galin L.A. 1946 Spatial contact problems of the theory of elasticity for punches of circular shape in planar projection. *PMM J. Appl. Math. Mech.*, **10**, 425–448. (Russian)

[5] Borodich F.M. 2008 Hertz type contact problems for power-law shaped bodies. In: *L.A. Galin, Contact Problems. The Legacy of L.A. Galin (G.M.L. Gladwell Ed.)*, Springer, 261–292.

[6] Bradley R.S. 1932 The cohesive force between solid surfaces and the surface energy of solids. *Phil. Mag*, **13**, 853–862.

[7] Derjaguin B. 1934 Untersuchungen über die Reibung und Adhäsion, IV. Theorie des Anhaftens kleiner Teilchen. *Kolloid Zeitschrift*, **69**, 155–164.

[8] Sperling G. 1964 Eine Theorie der Haftung von Feststoffteilchen an festen Körpern. Dissertation, Technische Hochschule Karlsruhe.

[9] Johnson K.L. 1958 A note on the adhesion of elastic solids. *Brit. J. Appl. Phys.*, **9**, 199–200.

[10] Johnson K.L., Kendall K. and Roberts A.D. 1971 Surface energy and the contact of elastic solids.*Proc. R. Soc. Lond. A*, **324**, 301–313.

[11] Kendall K. 2001 *Molecular Adhesion and Its Applications.* Kluwer Academic/Plenum Publishers, New York.

[12] Barthel E. 2008 Adhesive elastic contacts: JKR and more.*Journal of Physics D: Applied Physics*, **41**(16), 1630013.

[13] Galanov B.A. 1993 Development of analytical and numerical methods for study of models of materials. Report for the project 7.06.00/001-92, 7.06.00/015-92. Institute for Problems in Materials Science, Kiev. (Ukrainian)

[14] Galanov B.A. and Grigor'ev O.N. 1994 Adhesion and wear of diamond. Part I. Modelling. Preprint. Institute for Problems in Materials Science., Nat. Ac. Sci. Ukraine, Kiev.

[15] Carpick R.W., Agraït N., Ogletree D.F. and Salmeron M. 1996 Measurement of interfacial shear (friction) with an ultrahigh vacuum atomic force microscope. *J. Vac. Sci. Technol. B*, **14**, 1289–1295.

[16] Borodich F.M., Galanov B.A., Keer L.M. and Suarez-Alvarez M.M. 2014 The JKR-type adhesive contact problems for transversely isotropic elastic solids. *Mechanics of Materials*, **75**, 34–44

[17] Borodich F.M., Galanov B.A. and Suarez-Alvarez M.M. 2014 The JKR-type adhesive contact problems for power-law shaped axisymmetric punches. *J. Mech. Phys. Solids*, **75**,14–32

[18] Griffith A.A. 1920 The phenomena of rupture and flow in solids. *Phil. Trans. R. Soc.*, (London), **A221**, 163-198.

[19] Borodich F.M. and Galanov B.A. 2016 Contact probing of stretched membranes and adhesive interactions: Graphene and other two-dimensional materials. *Proc. Royal Society A: Mathematical, Physical and Engineering Sciences*, **472(2195)**, 2016.0550

[20] Borodich F.M., Galanov B.A., Perepelkin N.V. and Prikazchikov D.A. 2019 Adhesive contact problems for a thin elastic layer: Asymptotic analysis and the JKR theory. *Mathematics and Mechanics of Solids*, **24(5)**, 1405–1424.

[21] Erbaş B., Aydın Y.E., Borodich F.M. 2019 Indentation of thin elastic films glued to rigid substrate: Asymptotic solutions and effects of adhesion. *Thin Solid Films*, **683**, 135-143

[22] Shull K.R., Ahn D., Chen W.-L., Flanigan C.M. and Crosby A.J. 1998 Axisymmetric adhesion tests of soft materials.*Macromol. Chem. Phys.*, **199**, 489–511

[23] Shull K.R 2002 Contact mechanics and the adhesion of soft solids. *Mat. Sci. Eng. R: Reports*, **36(1)**, 1–45.

[24] Popov V.L. 2018 Solution of adhesive contact problem on the basis of the known solution for non-adhesive one.*Facta Universitatis: Mechanical Engineering,***49(4)**, 93-98

[25] Argatov I., Li Q., Pohrt R. and Popov V.L. 2016 Johnson–Kendall–Roberts adhesive contact for a toroidal indenter. *Proc. R.Soc. Lond. A*, **472**, 20160218.

[26] Sridhar I, Johnson K L. and Fleck N. A. 1997 Adhesion mechanics of the surface force apparatus. *J. Phys. D: Appl. Phys.* **30**, 1710–1719

[27] Johnson K.L. and Sridhar I. 2001 Adhesion between a spherical indenter and an elastic solid with a compliant elastic coating. *J. Phys. D: Appl. Phys.*, **34**, 683

[28] Sridhar I., Zheng Z.W. and Johnson K.L. 2004 A detailed analysis of adhesion mechanics between a compliant elastic coating and a spherical probe. *J. Phys. D: Appl. Phys.*, **37**, 2886–2895

[29] Rostovtsev N.A. 1953 Complex stress functions in the axisymmetric contact problem of elasticity theory. *PMM J. Appl. Math. Mech.*, **17**, 611–614.

[30] Sneddon I. 1965 The relation between load and penetration in the axisymmetric boussinesq problem for a punch of arbitrary profile. *Int. J. Engng Sci.*, **3**, 47–57.

[31] Willis J.R. 1966 Hertzian contact of anisotropic bodies. *J. Mech. Phys. Solids*, **14**, 163–176.

[32] Conway H.D., Farnham K.A., Ku T.C. 1967 The indentation of a transversely isotropic half space by a rigid sphere. *J. Appl. Mech.*, **34(2)**, 491–492.

[33] Timoshenko S. and Woinowsky-Krieger S. 1959 *Theory of plates and shells.* McGraw–Hill, New York.

[34] Argatov I. and Mishuris G. 2015 *Contact Mechanics of Articular Cartilage Layers. Asymptotic Models.* Springer.

[35] Winkler E. 1867 *Die Lehre von der Elastizität und Festigkeit, mit Besonderer Rücksicht auf ihre Anwendung in der Technik, für Polytechnische Schulen, Bauakademien, Ingenieure, Maschinenbauer, Architekten, etc.* Verlag H. Dominicus, Prague

[36] Pasternak P.L. 1954 *On a new method of analysis of an elastic foundation by means of two foundation constants.* Gosudarstvennoe Izdatelstvo Literaturi po Stroitelstvu i Arkhitekture, Moscow (Russian).

[37] Filonenko-Borodich M.M. 1940 Some approximate theories of the elastic foundation. *Uchenyie Zapiski Moskovskogo Gosudarstvennogo Universiteta. Mekhanika*, **46**, 3–18 (Russian).

[38] Ansys Theory Reference: Element Library. Element CONTA175. Available online: https://ansyshelp.ansys.com/account/secured?returnurl=/Views/Secured/corp/v194/ans_elem/Hlp_E_CONTA175.html

[39] Borodich F.M. and Galanov B.A. 2008 Non-direct estimations of adhesive and elastic properties of materials by depth-sensing indentation. *Proc. R. Soc. Ser. A*, **464**, 2759–2776.

[40] Perepelkin N.V., Kovalev A.E., Gorb S.N. and Borodich F.M. 2019 Estimation of the elastic modulus and the work of adhesion of soft materials using the extended Borodich-Galanov (BG) method and depth sensing indentation. *Mech. Mat.*, **129**, 198–213.

[41] Perepelkin N.V., Argatov I.I. and Borodich F.M. 2019 Evaluation of elastic and adhesive properties of solids by depth-sensing indentation. *The Journal of Adhesion*, DOI: 10.1080/00218464.2019.1686981

[42] Perepelkin N.V., Borodich F.M., Kovalev A.E. and Gorb S.N. 2020 Depth-Sensing Indentation as a Micro- and Nanomechanical Approach to Characterisation of Mechanical Properties of Soft, Biological, and Biomimetic Materials. *Nanomaterials*, **10(1)**, 15.

[43] Perepelkin N.V. and Borodich F.M. 2019 Evaluation of elastic and adhesive properties of protective coatings. 7th European Conference on Tribology ECOTRIB2019 (12-14 June 2019, Vienna, Austria): Book of Abstracts. ISBN 978-3-901657-60-3.

[44] Ciavarella M. 2018 An approximate JKR solution for a general contact, including rough contacts, *J. Mech. Phys. Solids*, **114**, 209–218.

[45] Heß M. and Forsbach F. 2020 Macroscopic Modeling of Fingerpad Friction Under Electroadhesion: Possibilities and Limitations. *Frontiers in Mechanical Engineering*, **6**, 2020, 567386.

[46] Argatov I., Heß M., Pohrt R. and Popov V. 2016 The extension of the method of dimensionality reduction to non-compact and non-axisymmetric contacts. Z. Angew. Math. Mech., 96, 1144-1155.

[47] Argatov I., Heß M. and Popov V.L. 2018 The extension of the method of dimensionality reduction to layered elastic media. Z. Angew. Math. Mech., 98, 622-634.

Appendix A

In this Appendix, we consider a numerical example which has a twofold purpose. On the one hand, the example demonstrates the accuracy of the approach to numerical reconstruction of parametric force-displacement curves based on the combination of a Boussinesq-type model and a Hertz-type model described in Section 5. On the other hand, it demonstrates that the two properties of slopes of force-displacement curves discussed earlier are valid and can be easily implemented for Finite Element Method (FEM) calculations.

The example is based on a FE model of an elastic bi-layer structure (a disk) bonded to a rigid base at the bottom and on the outer edge (Fig. 8). When the diameter-to-thickness ratio is high, such a model can approximate the elastic response of an infinite bi-layer structure bonded to a rigid base.

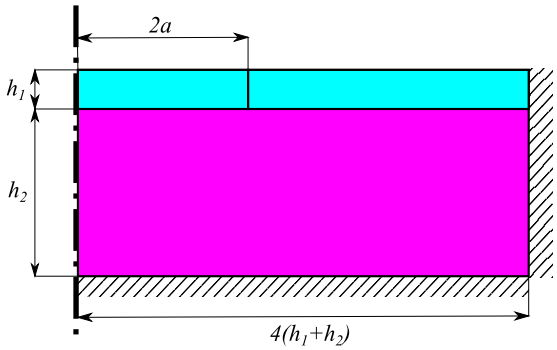

Figure 8: Geometrical model of a bi-layer disk.

Three contact problems involving this elastic structure were considered using the Ansys Mechanical APDL 2019 and Matlab 2019 software. *Problem 1*: a Boussinesq-type contact problem involving a circular cylindrical indenter of radius a; *Problem 2*: a Hertz-type contact problem involving a spherical indenter of radius R; *Problem 3*: a verification contact problem (identical to No.2 but with a different indentation depth, see the details below).

In a sequence of steps, we assigned the value of the contact radius $a = a^*$, then identified the corresponding slope value using a Boussinesq-type model, then assumed the same slope value in the Hertz-type problem and identified the respective values of indentation depth $\delta = \delta^*$ and force $P = P^*$. As a verification step, the value of the contact radius corresponding to $\delta = \delta^*$ was evaluated directly from FEM model, thus making the complete circle in the diagram in Fig. 7. The final value of a was then compared with the initially set one. The calculations were done as follows.

Step 1. A particular value $a = a^*$ was set for the radius of the cylindrical indenter in Problem 1, and a force-displacement relation was numerically obtained in Ansys as a set of discrete values corresponding to different loading substeps.

Step 2. In Problem 2, a force-displacement relation for the same medium and the spherical indenter was numerically obtained in Ansys, again in discrete form as pairs of force and displacement values.

According to the proofs in Section 3, the force-displacement relation in Step 1 should be linear and have exactly the same slope as the force-displacement relation in Step 2 when the contact radius in the latter reaches the value a^*.

Step 3. Using Matlab, the discrete force-displacement data from Problem 1 was least-squares fitted with a straight line and the slope value S^* was extracted. The discrete force-displacement data for Problem 2 was least-squares fitted with B-splines using Matlab's spap2 routine and then differentiated thus obtaining slope values S corresponding to individual (P, δ) points. That data was then re-arranged by means of another spline fitting in the form of the following dependencies: $\delta = \delta(S), P = P(S)$. Finally, the value $S = S^*$ from Step 1 was substituted into the latter dependencies to evaluate the values of the indentation depth $\delta^* = \delta(S^*)$ and the indentation force $P^* = P(S^*)$ which correspond to the slope value S^* and the contact radius value a^*.

Step 4 (Verification). To verify the results of Step 3, Problem 3 identical to Problem 2 was considered. The only difference was that the final indentation depth was now set to δ^*. Then the respective values of the indentation force and the contact radius were identified directly from the FEM results and compared to the values a^* and P^* from Steps 1-3.

The particular model parameters and calculation settings were as follows. The top layer had thickness $h_1 = 0.1$ mm and elastic properties: Young's modulus $E_1 = 3$ MPa, Poisson ratio $\nu_1 = 0.3$; the bottom layer had thickness $h_2 = 1.9$ mm and elastic properties: Young's modulus $E_2 = 300$ MPa, Poisson ratio $\nu_2 = 0.3$. The radius of the structure was $4(h_1 + h_2)$. The radius of the cylindrical indenter was set $a^* = 0.4$ mm, and the radius of the spherical one was $R = 10$ mm.

The FEM model for the bi-layer used in Steps 1,2, and 4 consisted of PLANE183 elements in axisymmetric formulation (with Ansys X-axis representing the radial coordinate). A part of the top layer of radius $2a = 0.8$ mm was meshed with quadrilateral mesh, the remaining parts of the model were meshed with free triangilar mesh. Note that making the finest mesh was not our goal in that exercise. A frictionless contact pair was made using

TARGE169 and CONTA175 elements. The indenter, be it cylindrical or spherical, became rigid target surface with a pilot node. The FEM model for Steps 2 and 4 is shown in Fig. 9.

Indentation depths in Steps 1 and 2 were arbitrary set 0.025 mm. Indentation displacement was applied as a kinematic constraint to the pilot node; indentation force was obtained as negative of the reaction value at that node using the time history post-processor POST26 in Ansys. All the Ansys simulations had the same number of 20 loading substeps. All the indentation data sequences were adjoined with zero data values corresponding to the moment of initial contact.

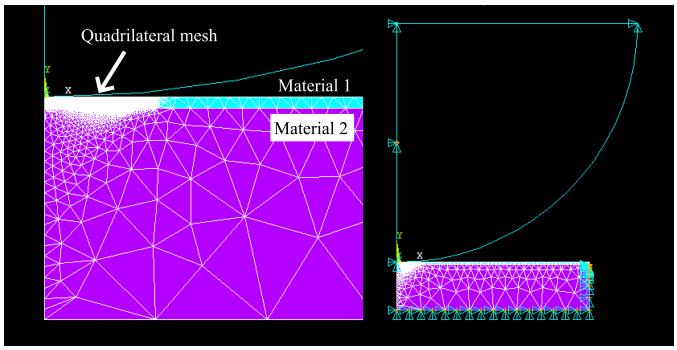

Figure 9: Finite element model of a bi-layer structure and a rigid spherical indenter.

The calculated results were as follows. The force-displacement data obtained in Step 1 (cylindrical indenter) for inenter radius $a^* = 0.4$ mm and indentation depth 0.025 mm was fitted, using Matlab, with the following straight line: $P = 20276.40623376623\delta - 0.00061455411$, hence $S^* = 20276.40623376623$ N/m. Using spline interpolation and numerical differentiation in Matlab, a point on the Step 2 force-displacement curve was identified, where the slope value was identical to S^*. The corresponding values of indentation depth and indentation force were: $\delta^* = 8.770177786585117 \cdot 10^{-03}$ mm, $P^* = 0.090008569091328$ N.

At the verification step, indentation depth for the spherical indenter was set to $\delta^* = 8.770177786585117 \cdot 10^{-03}$ mm. The corresponding value of the indentation force was evaluated in Ansys as 0.0899206 N. Compared with the value of P^*, this shows the relative error of 0.0977341%. Next, the contact radius was approximated directly from the Ansys output by finding the outermost contact node indicating the closed contact status, which gave the value of 0.402 mm, whereas the theoretically predicted value was the initially set $a^* = 0.4$ mm. Hence, the relative error was 0.5%.

Thus, despite its increased complexity, the two-model approach to reconstructing parametric force-displacement dependency exhibits its high accuracy. The above example also demonstrates the fact that the properties of slopes of force-displacement curves discussed in Section 3 are applicable to FEM calculations as well.